Computers and Fluids 164 (2018) 64–72

Contents lists available at ScienceDirect

Computers and Fluids

journal homepage: www.elsevier.com/locate/compfluid

The study on interface characteristics near the metal wall by a molecular dynamics method

Lei Chen, Peng-Fei Chen, Zhong-Zhen Li, Ya-Ling He, Wen-Quan Tao*

Key Laboratory of Thermo-Fluid Science and Engineering, Ministry of Education; School of Energy & Power Engineering, Xi'an Jiaotong University, Xi'an, Shaanxi, People's Republic of China, 710049

ARTICLE INFO

Article history:
Received 17 February 2016
Revised 2 March 2017
Accepted 9 March 2017
Available online 10 March 2017

Keywords:
Molecular dynamics
Solid wall
Interface characteristic
Condensation process
Materials studio
Three-phase model

ABSTRACT

The condensation process of the multiple-atom and polar water molecular at a solid wall is studied. It is found that a monomolecular layer structure is existed on the wall surface and the intensity of solid-liquid potential can be revealed by the monomolecular density peak. At high-temperature conditions, liquid drop in vapor and bubble near wall can be observed. The solid-liquid potential energy on monomolecular layer structure has a greater impact than on gas-liquid interface. The simulated densities in the vapor region are consistent with the macroscopic values by refprop8.0, while in the liquid region the simulated densities are a bit lower than the macroscopic ones. Besides, the solid-liquid-gas three-phase model consisting of argon, water, freon and copper was constructed using Materials Studio software, and their interface characteristics are studied.

1. Introduction

Water is widely applied in the fields of science and engineering as a working fluid in the heat and mass transfer process. For many interfacial phenomena, such as water film condensation and drop wise condensation, investigations are still stuck on the semi-empirical level due to the great difficulties encountered in detail experimental study. Now, many scholars began to reveal the nature of water, gas-liquid interface characteristics using the molecular simulation technology [1–5].

The water molecule is polyatomic molecule with a more complex structure than the monatomic molecule; meantime, it is polar molecule, so the long-range electrostatic force is existed among the molecules. To simulate the movement of water molecule, the translational, autorotation and polarity caused by the electrostatic interactions can't be neglected. There are mainly SPC, SPC/E, TIP3P, TIP4P and TIP5P models to simulate the water molecule, and the thermodynamic parameters obtained by SPC/E and TIP4P models are in good agreement with the experimental values [6–8] in a large temperature variation range.

There have been numerous reports [1–13] about the characteristics of the water near the wall, but there is no particularly accurate model to describe the structure of water molecules and the interaction between water and platinum. In this paper, a gas-liquid -solid three-phase model is constructed to simulate vapor-liquid equilibrium near the wall and to study the interface characteristics.

Although, in recent years, a great progress in the interface characteristics studies has been made using molecular dynamics simulation [12–21], but only water and platinum are involved in the above research. The working fluid and metal material involved in the previous studies are quite limited for it is difficult to obtain the force field between them. For example, Freon is widely used in small food banks, household refrigerators, and water and copper are commonly used in heat exchangers. But there are very limited studies on them in the literature. So in this paper, the solid-liquid-gas three-phase model consisting of argon, water, freon and copper will be constructed using Materials Studio software, and their interface characteristics will be studied.

2. Simulation details of water-platinum system

2.1. Molecular model and potential function

In the simulation, SPC/E and TIP4P model are adopted and the ZP and the SH potential functions [10] are used to describe the interactions between water and platinum.

SPC/E and TIP4P models both are the planar structure (i.e. oxygen atom, hydrogen atom, and negative charge are in the same plane). In fact, SPC/E is flat three-point model, and TIP4P is plane four-point model. The water molecule structures of the

* Corresponding author.
E-mail addresses: chenlei@mail.xjtu.edu.cn (L. Chen), wqtao@mail.xjtu.edu.cn (W.-Q. Tao).

http://dx.doi.org/10.1016/j.compfluid.2017.03.013
0045-7930/

Nomenclature

c[-]	[-]The unit vector of the specific rotational axis
[-]	Torque
q[C]	Charge
r[m]	Distance
r_c[m]	Truncation radius
R[-]	Conversion matrix between the two coordinate systems
w[-]	Orthogonal antisymmetric matrices

Special characters

α[-]	Lagrange factor
ε_{RF}[-]	Dielectric constant
ϕ[-]	First Euler angle
φ[-]	Second Euler angle
θ[-]	Third Euler angle
ρ[-]	Projection of distance vector on the surface
ζ[-]	Rotation angle

Subscripts

a	Interacting molecule
b	Interacting molecule
i	Molecule position
j	Molecule position

two models are shown in Fig. 1, where O, H, and L represent the location of the oxygen atom, hydrogen atom, and negative charge, respectively. The characteristic parameters of the different models are in Table 1.

In the different models, the spatial structure of the water molecule is different, but their potential functions can be expressed by a unified form as follows:

$$u_{ab}(r_{ij}) = u_{LJ}(r_{ij}) + u_{coul}(r_{ij}) = 4\varepsilon\left[\left(\frac{\sigma}{r_{oo}}\right)^{12} - \left(\frac{\sigma}{r_{oo}}\right)^{6}\right] + \sum_{i\in a}\sum_{j\in b}\frac{q_i q_j}{r_{ij}} \quad (1)$$

Where, $a$and$b$represent the interacting molecules; $r_{ij}$is the distance between $a$at the i position and $b$at the j position; q_i, $q_j$are the charges they carried at i, j position, respectively; $r_{oo}$is the distance of oxygen-oxygen. $i \in a$indicates that the i-th atom or charge of$a$. In Eq. (1), the first term on the right is the short-range LJ potential and the second term is the long-range electrostatic interaction potential. Short-range potential is considered by a large truncation radius, for example:3.5σ; the reaction field treatment [19] is adopted for the long-range potential. The electrostatic potential can be written as:

$$u_{coul}(r_{ij}) = \sum_{i\in a}\sum_{j\in b}\frac{q_{iq_j}}{r_{ij}}\left[1 + \frac{\varepsilon_{RF-1}}{\varepsilon_{RF}+1}\left(\frac{r_{ij}}{r_c}\right)\right] \quad (2)$$

where, $r_c$is truncation radius; $\varepsilon_{RF}$is dielectric constant.

In Eq. (2), the dielectric constant is taken to be infinite in the computation, and the latter part of the right bracket is the reaction field interaction, which means that the difference between the Coulomb force and the reaction field force is reduced to zero when the distance of the charged atoms is close to the critical cutoff radius.

2.2. The fourth-order moment method

In the simulation, water molecule will be generally treated as a rigid body. Rigid motion can be decomposed into two separate parts: the translation along the centroid and the rotation around the centroid. The translation of rigid molecule is controlled by the external force, and the rotation is dependent on the torque suffered. So two coordinate systems of the rigid body dynamics: space fixed coordinate system and space moving coordinate system will be used. Keep coordinate system invariable and fix the moving coordinate system with the rigid body. Its origin always lies at the molecular centroid, translating and rotating with molecule. So, for every molecule, its location in the moving coordinate system is invariable. But the motion coordinate system is always changing, so the physical quantities in the moving coordinate system should be converted into those in the space fixed coordinate system while calculating. Generally, the fourth moment method [1, 6–8] is adopted to establish the conversion between the two coordinate systems.

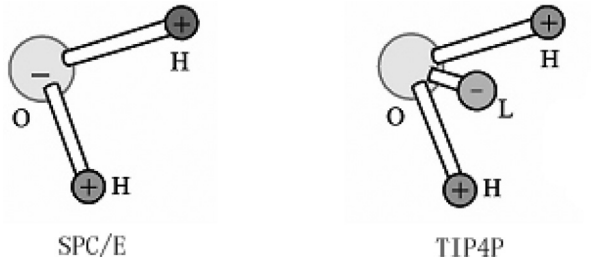

Fig. 1. Water molecule model.

Table 1
Geometrical and physical parameters of water molecule.

	q_H/e	σ/nm	$\varepsilon \cdot k_B^{-1}$/K	r_{OH}/nm	θ_{HOH}/°	r_{OL}/nm
SPCE	0.4238	0.31656	78.2	0.1	109.47	–
TIP4P	0.52	0.315365	78.08	0.09572	104.52	0.015

Define the fourth moment $Q = (q_1, q_2, q_3, q_4)$, $(\theta,\ \phi,\ \varphi)$the Eulerspatial angle, R the conversion matrix between the two coordinate systems.

Let:

$$\begin{aligned} q_1 &= \sin(\theta/2)\cos((\phi-\varphi)/2) \\ q_2 &= \sin(\theta/2)\sin((\phi-\varphi)/2) \\ q_3 &= \cos(\theta/2)\sin((\phi+\varphi)/2) \\ q_4 &= \cos(\theta/2)\cos((\phi+\varphi)/2) \end{aligned} \quad (3)$$

where, $\sum_m q_m^2 = 1$,

$$\begin{aligned} \sin\theta &= 2\sqrt{(q_1^2+q_2^2)(1-q_1^2-q_2^2)} \\ \cos\theta &= 1-2(q_1^2+q_2^2) \\ \sin\phi &= 2(q_1q_3+q_2q_4)/\sin\theta \\ \cos\phi &= 2(q_1q_4-q_2q_3)/\sin\theta \\ \sin\varphi &= 2(q_1q_3-q_2q_4)/\sin\theta \\ \cos\varphi &= 2(q_1q_4+q_2q_3)/\sin\theta \end{aligned}$$

And any rotating around fixed point can be expressed as follows:

$$r' = r\cos\zeta + (c\cdot r)c(1-\cos\zeta) + (c\times r)\sin\zeta$$

where, c is the unit vector of the specific rotational axis; $\zeta$is rotation angle.

If $m = 1, 2, 3$, $q_m = c_m\sin(\zeta/2)$,$q_4 = \cos(\zeta/2)$, we get:

$$r' = (2q_4^2-1)r + 2(q\cdot r)q + 2q_4 q + 2q_4 q\times r$$

Define $r' = Rr$, we get:

$$R = 2\begin{pmatrix} q_1^2+q_4^2-\frac{1}{2} & q_1q_2+q_3q_4 & q_1q_3-q_2q_4 \\ q_1q_2-q_3q_4 & q_2^2+q_4^2-\frac{1}{2} & q_2q_3+q_1q_4 \\ q_1q_3+q_2q_4 & q_2q_3-q_1q_4 & q_3^2+q_4^2-\frac{1}{2} \end{pmatrix}$$

For non-linear motion equations of water molecules, the angular velocity and the fourth moment vector Q relationship is as

following:

$$\begin{pmatrix}\omega_x'\\ \omega_y'\\ \omega_z'\\ 0\end{pmatrix} = 2W\begin{pmatrix}\dot{q}_1\\ \dot{q}_2\\ \dot{q}_3\\ \dot{q}_4\end{pmatrix} \tag{4}$$

where, W is the orthogonal antisymmetric matrices.

$$W = \begin{pmatrix} q_4 & q_3 & -q_2 & -q_1\\ -q_3 & q_4 & q_1 & -q_2\\ q_2 & -q_1 & q_4 & -q_3\\ q_1 & q_2 & q_3 & q_4\end{pmatrix} \tag{5}$$

For space fixed coordinate system, torque is equal to the change rate of angular momentum, i.e.

$$N = \frac{dL}{dt} \tag{6}$$

Due to conversion relationship of the fixed coordinate system and moving coordinate system:

$$\left(\frac{dL}{dt}\right)_{fixed} = \left(\frac{dL}{dt}\right)_{moving} + \omega \times L$$

So, in moving coordinate system, Eq. (6) is turned into:

$$N_x = \dot{L}_x + \omega_y' L_z - \omega_z' L_y$$

Concidering $L_x = I_x\omega_x'$, we get the Euler equation of motion coordinate:

$$I_x\dot{\omega}_x' = N_x + (I_y - I_z)\omega_y'\omega_z' \tag{7}$$

So does to the other two directions.

Through torque convert from space fixed coordinate system to moving coordinate system, the acceleration is obtained. The vector form is as follows:

$$\begin{pmatrix}\ddot{q}_1\\ \ddot{q}_2\\ \ddot{q}_3\\ \ddot{q}_4\end{pmatrix} = \frac{1}{2}W^{\mathrm{T}}\begin{pmatrix}\dot{\omega}_x'\\ \dot{\omega}_y'\\ \dot{\omega}_z'\\ -2\sum \dot{q}_m^2\end{pmatrix} \tag{8}$$

The above formula is to calculate the conversion when the water molecules rotate, and the specific implementation program is as following:

(1) Fix every action spot in the selected molecule model at the coordinate of the model center, and calculate the position force and torque.
(2) Given rotation inertia I, arbitrarily select Euler angles, and initialize$\dot{q}_i (i = 1, 2, 3, 4)$.
(3) According to Eq. (3), compute$\dot{q}_i (i = 1, 2, 3, 4)$.
(4) According to Eqs. (4, 5), compute$\omega_x', \omega_y', \omega_z'$.
(5) According to Eq. (7), compute$\dot{\omega}_x', \dot{\omega}_y', \dot{\omega}_z'$
(6) According to Eq. (8), compute$\ddot{q}_i (i = 1, 2, 3, 4)$, and finally, compute distance.
(7) Repeat (3)–(6), until the balanced outputs.

2.3. Potential model of water-platinum

In this paper, two different kinds of potential functions are adopted to describe the interaction between water molecule and platinum surface, which are both developed from Huckel's water molecule and platinum cluster model. One of them is the SH model, which is put forword by Spohr and Heinzinger at 1988. And at 1989, Spohr studied the structure of water on the platinum surface by the solid-liquid potential function [11]. Mathematical

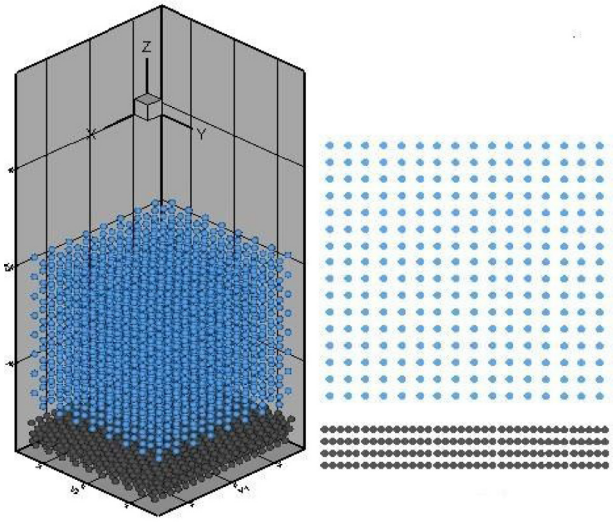

Fig. 2. Initial state of simulated system.

description of the S-H potential is as follows:

$$\begin{aligned} u_{H_2O-Pt} &= u_{O-Pt}(r_{O-Pt}, \rho_{O-Pt}) + u_{H-Pt(r_{H_1-Pt})} + u_{H-Pt(r_{H_2-Pt})}\\ u_{O-Pt}(r_{O-Pt}, \rho_{O-Pt}) &= 7.9\exp(-1.1004r)f(\rho)\\ &\quad +10^6\exp(-5.3568r)[1 - f(\rho)]\\ u_{H-Pt(r_{H-Pt})} &= 1.7142\exp\left(-0.5208\rho^2\right) = 1.7142f(\rho) \end{aligned} \tag{9}$$

where, the energy unit is 10^{-19}J, the length unit is angstrom (Å). $r$is the distance between the different location points among molecules; $\rho$is projection of distance vector on the surface. The results from Eq. (9) show that when the distance is in 2–10Å, the metal surface attracts water molecules because of the role of the induced charge, and when the distance is more than 10 Å, potential become very small. So in SH potential the cutoff radius can be chosen greater than 10Å. In this paper, the cutoff radius selected is about 11Å. Another one is ZP model [12] developed by Zhu and Philpott in 1994. The potential function includes the electrostatic interaction potential of the water molecules and the wall, isotropic and anisotropic short-range interaction potential, and it is expressed as:

$$\begin{aligned} u_{H_2O-surf} &= u_{H_2O-cond} + u_{an}(O, r_O) + u_{isr}(O, r_O)\\ &\quad + \sum_H [u_{an}(H, r_H) + u_{isr}(H, r_H)] \end{aligned} \tag{10}$$

$$u_{H_2O-cond} = \sum_{l,k} \frac{q_l q_k}{2r_{lk}} \tag{11}$$

For a point particle p, we have

$$u_{an}(p, r_p) = 4\varepsilon_{p-Pt}\sum_j \left[\left(\frac{\delta_{p-Pt}^2}{(\alpha\rho_{pj})^2 + z_{pj}^2}\right)^6 - \left(\frac{\delta_{p-Pt}^2}{(\rho_{pj}/\alpha)^2 + z_{pj}^2}\right)^3\right] \tag{12}$$

$$u_{isr}(p, r_p) = -4\varepsilon_{p-Pt}\sum_j \frac{c_{p-Pt}\delta_{p-Pt}^{10}}{r_{pj}^{10}} \tag{13}$$

where,

$$\begin{aligned} \alpha &= 0.8\\ \delta_{O-Pt} &= 0.27\text{nm}, \varepsilon_{O-Pt} = 6.44 \times 10^{-21}\text{J}, c_{O-Pt} = 1.28\\ \delta_{H-Pt} &= 0.255\text{nm}, \varepsilon_{H-Pt} = 3.91 \times 10^{-21}\text{J}, c_{H-Pt} = 1.2 \end{aligned}$$

$u_{H_2O-cond}$is molecular-conduction electron potential; $u_{an}(p, r_p)$is anisotropic short-range potential; $u_{isr}(p, r_p)$is isotropic short-range potential.

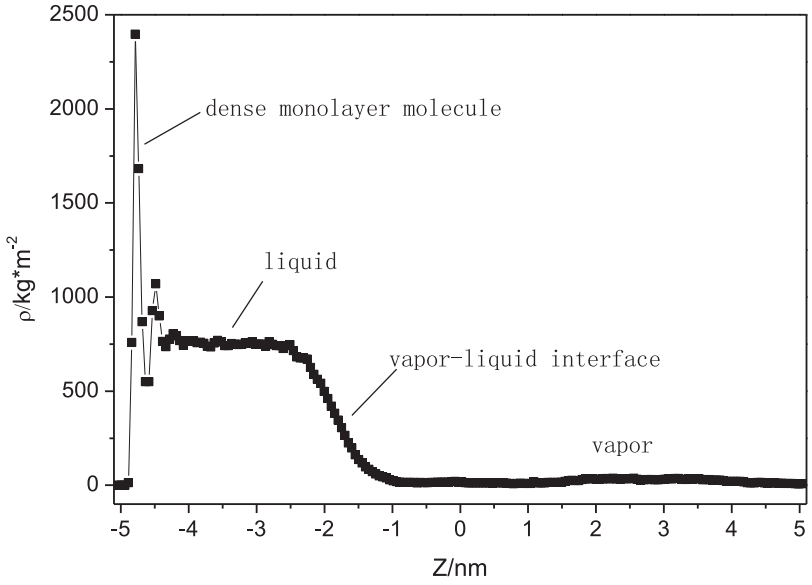

Fig. 3. Density distribution of the system (500 K, SPCE/S-H model).

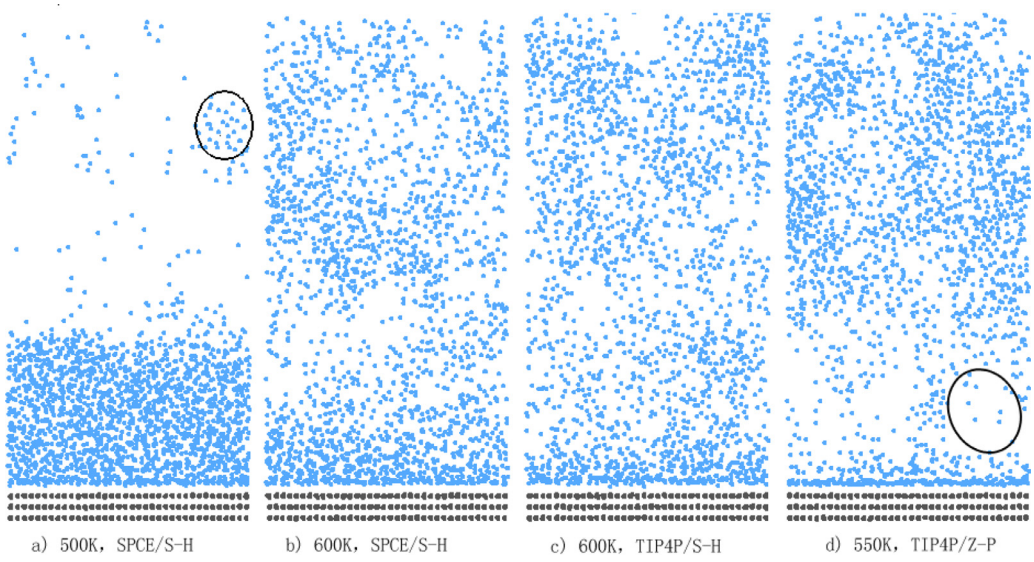

Fig. 4. Water molecular positions at the different conditions.

2.4. Molecular dynamic simulation

The initial position of the water molecules are arranged at the lower part of simulation area in a face-centered cubic, and the bottom of system is solid wall [20]. Fig. 2 shows the initial structure. Solid wall is composed of 1800 Pt atoms and there are 2048 molecule in fluid zone. In order to prevent the water molecules and the platinum atoms too close leads to calculating overflow, the distance between the bottom water molecules and the wall is about 0.63 nm. Periodic boundary condition is adopted around the simulation region, and mirror boundary condition is adopted in the top and bottom. The moment of inertia of water molecule is very small, and water molecule rotates at high speed when moving, so in order to keep the stability of the system, the time step is 0.5fs; integral format of motion equations is prediction-correction format; the solid wall temperature is controlled by image molecules; maintain temperature of the water molecules in the simulation system by constraint method, and the rotational kinetic energy of water molecules should be considered. So the total kinetic energy of the molecules in the system:

$$N_m E_k = \frac{1}{2}\sum_i \dot{r}_i^2 + \frac{1}{2}\sum_x I_x \sum_i \omega_{xi}^{\prime 2} \tag{14}$$

In order to keep the kinetic energy invariable, introduce constraint items and limit equations for each dimension of the equations of motion. Add a constraint for every molecule as follows:

$$m\ddot{r}_i = F_i + \alpha m\dot{r}_i$$

$$\sum_x I_x \dot{\omega}'_{xi} = N_i + \alpha \sum_x I_x \omega'_{xi}$$

where, α is lagrange factor.

In order to obtain the thermostat, keeping the total kinetic energy of the water molecules unchanged, i.e. $\dot{E}_k = 0$, the constraint

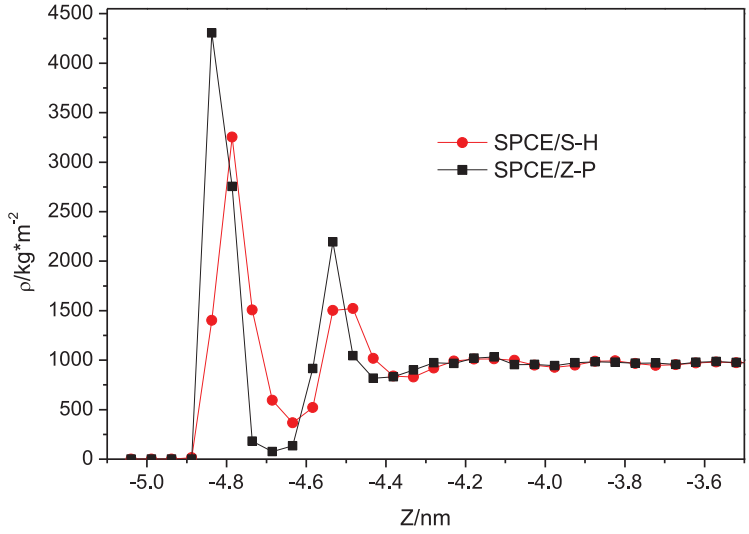

Fig. 5. Distribution of water density near the solid wall.

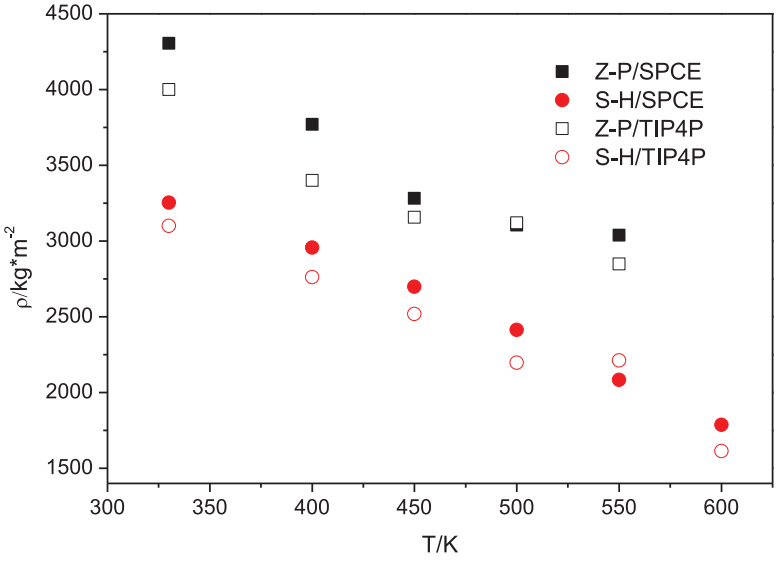

Fig. 6. Dependence of density peak of the first layer on the temperature.

factor can be obtained:

$$\alpha = -\frac{\sum_i \dot{r}_i \cdot F_i + \sum_i \omega_i' \cdot N_i}{m\sum_i \dot{r}_i^2 + \sum_x I_x \sum_i \omega_{xi}'^2}$$

In simulation, adjust system temperature once every 50 step to maintain a constant temperature; the system get to equilibrium in former 100 ps, and another 50 ps to calculate parameters we want to know. To compare the results of different models, interface parameters of four combinations (SPC/E and SH, the SPC/E and ZP, TIP4P and SH and TIP4P and ZP) are caculated.

3. Results and discussion

3.1. Water molecular position and density distribution

Fig. 3 is the density distribution of the water molecules in the simulation system. The simulation system temperature is 500 K, the water molecules adopt SPC/E model, and the potential function of water - platinum is SH function. It can be seen that there is the dense monolayer water molecule structure at z = 5.06 nm, whose density is approximately 3 times to the fluid zone. This is because the water-platinum potential near the wall surface is dominant, and the water molecules are adsorbed into the dense monolayer on the wall, which is called "monolayer" structure in literature [10].

The fluid above the monolayer structure can be divided into liquid zone, gas-liquid interface area and gas area. Fig. 4(a) shows the position distribution after equilibrium. There are water molecules condensing nucleation phenomenon in the gas area (shown by black circles in Fig. 4(a)), but this phenomenon in the lower temperature (330 K, 400 K, 450 K) is not obvious. This may be associated with the presence of the solid wall and the initial position. Since water molecules are relatively sparse at the start, and there are two molecular layers between the bottom of the water molecules and the wall. Because of the interaction between the water and the wall surface, when the water molecule hits the wall, "water droplets are splashed into the gas zone. At 600 K, it can be seen from Fig. 4(b), (c) that there is no obvious gas-liquid interface, and Fig. 4(d) shows at 550 K a large number of bubbles formed at wall surface.

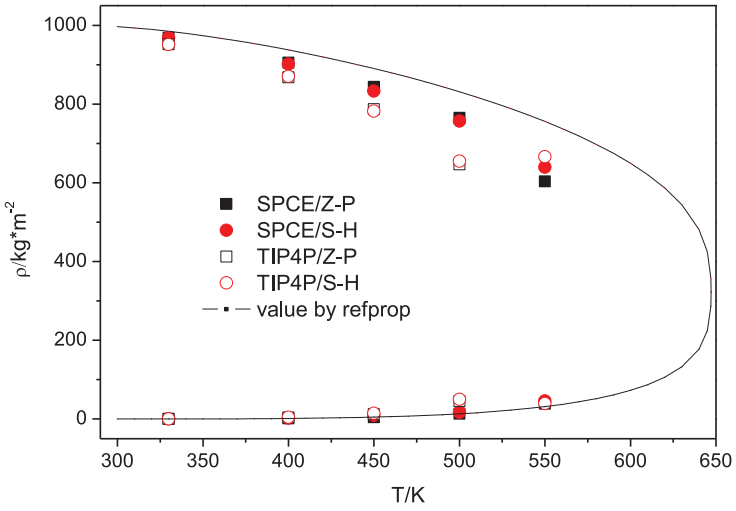

Fig. 7. Density and temperature of saturated water.

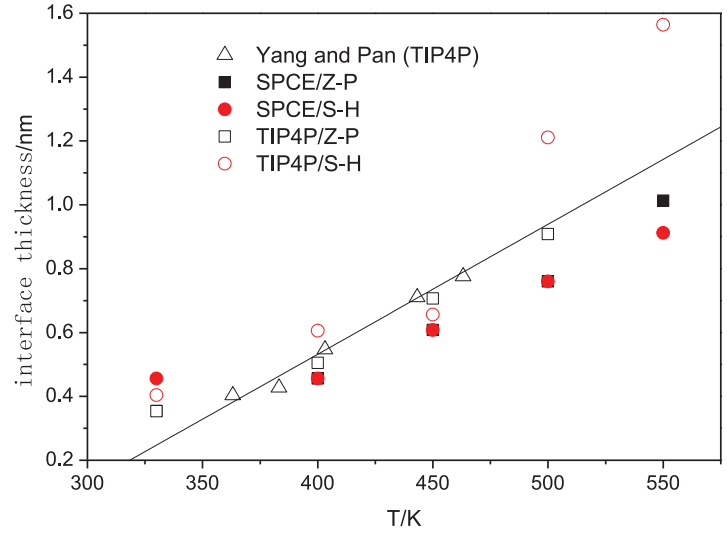

Fig. 8. Dependence of liquid-vapor interface width on the temperature.

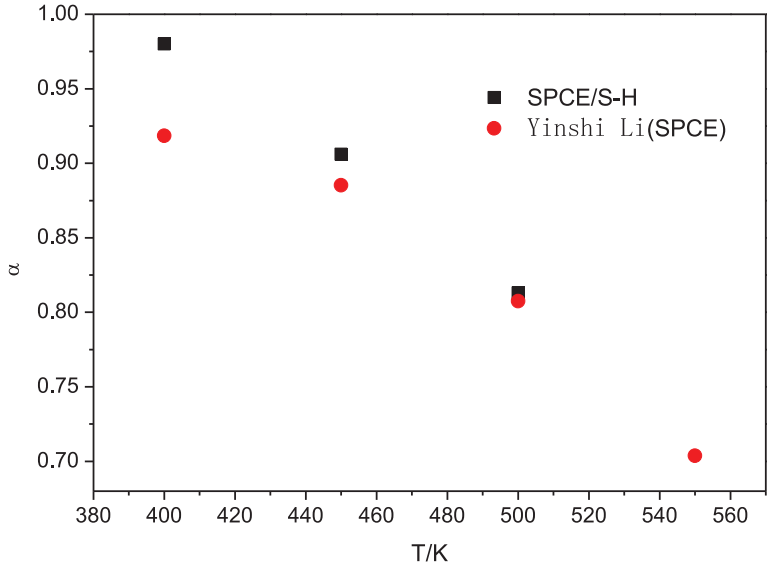

Fig. 9. Condensation coefficient.

3.2. Solid-liquid interfacial properties

Fig. 5 shows the molecular structure of water near the wall at 400 K. It can also be seen from the figure, about two molecules diameter (0.63 nm) thickness is between the wall surface and the density stabilized liquid molecules, and there are two significant density peaks. The density of the first layer water molecules obtained by ZP model is bigger and more close to the wall, which shows the ZP Potential is stronger than the SH Potential. It is consistent with the results of Kimura and Maruyama [10].

Fig. 6 shows that the density peak of the first layer water molecules on the wall surface varies with temperature. As the temperature increases, the kinetic energy of the water molecules, they break away more easily from the wall surface, so the density of the monolayer water molecules is reduced with increasing temperature. The density peak obtained by combining SPC/E and ZP is the maximum, and the density peak obtained by combining TIP4P and SH is the minimum. These are mainly because ZP Potential is stronger than SH Potential and the liquid structure from SPC/E model is more compact than fromTIP4P model.

3.3. Gas-liquid interfacial properties

We adopt the different models of the water molecule and the solid-liquid potential functions to compute the saturation density of the water molecules near wall. The results are shown in Fig. 7. Compared with macroscopic value calculated by Refprop 8.0, the density in the gas phase zone is in good agreement; but density obtained in the liquid region is a bit lower, and the deviation increases with increasing temperature. We can also see from the figure, water molecule model affects the saturation density enormously; but saturated density values obtained by the different solid-liquid potential models are almost the same. The density values obtained by the SPC/E water molecule model are closer to that calculated by Refprop. The results are consistent with the literature [8].

This paper also studied the variation of the thickness of the gas-liquid interface and condensation coefficient. The thickness of the gas-liquid interface is determined according to the "15–85″ rule [22].

$$\rho_V^* + \frac{15}{100}(\rho_L^* - \rho_V^*)$$
$$\rho_L^* + \frac{85}{100}(\rho_L^* - \rho_V^*) \tag{15}$$

"15–85″ rule is presented by Liu et al. They introduce the fractal theory into molecular dynamics to simulate gas-liquid interfacial characteristics. They assert the gas-liquid interface is a fractal surface, extract the fractal dimension, and bring forward the "15–85″ rule to determine the interface thickness by the study of the gas-liquid interface thickness and the fractal dimension. The so-called "15–85″ rule is based on Formula (15) in the interface region to determine the density range, and the width of the density region obtained in this range is the width of the interface.

Fig. 8 shows the variation of the width of the gas-liquid interface along with temperature. The solid line represents the interface thickness fitting straight line obtained by Yang and Pan using the two-phase model [23] without solid wall. The thickness of interfaces at different temperatures from simulation results are distributed at both sides of the fitting curve. In low temperature region, the results obtained by the TIP4P model are consistent with literature values, but interface thickness values obtained by the SPC/E model are slightly lower. As the temperature increases, the level activity of water molecule from TIP4P model is higher than from the SPC/E model, so the width of the interface obtained by the high-temperature region TIP4P model is wider.

In this paper, condensation coefficient is obtained by the incident molecule method [24]. After the system reaches the equilibrium, the gas molecules are issued into the gas-liquid interface, track the trajectory of energy change and location change, and then determine the physical process of forming molecule. Fig. 9 shows condensation coefficient obtained by the SPC/E model at different temperature. As the temperature increases, the condensation coefficient is reduced, which agrees with the results obtained by the two-phase model [21]. The condensation coefficients

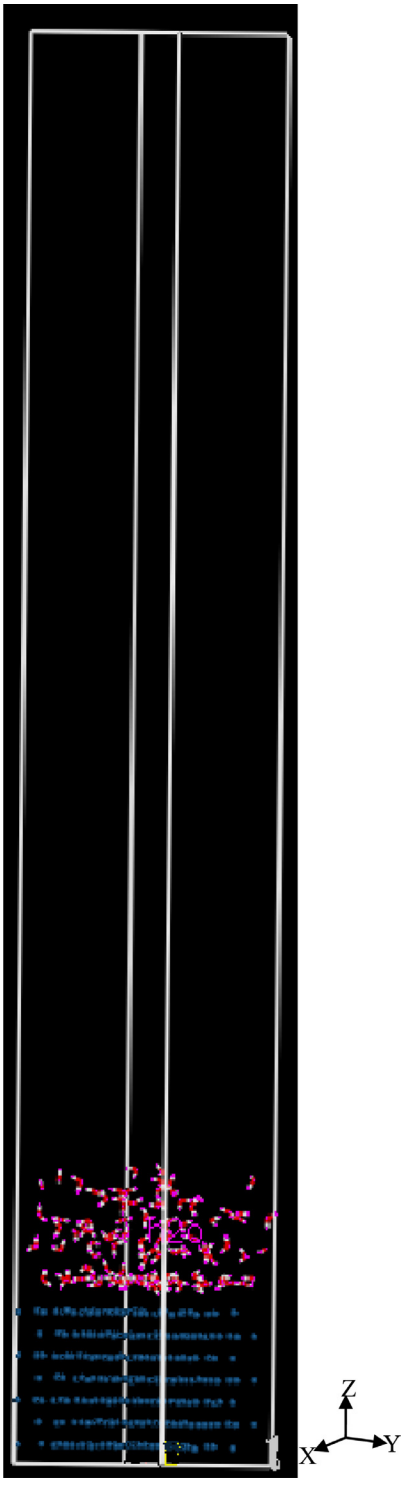

Fig. 10. The initial structure of Cu-H_2O system.

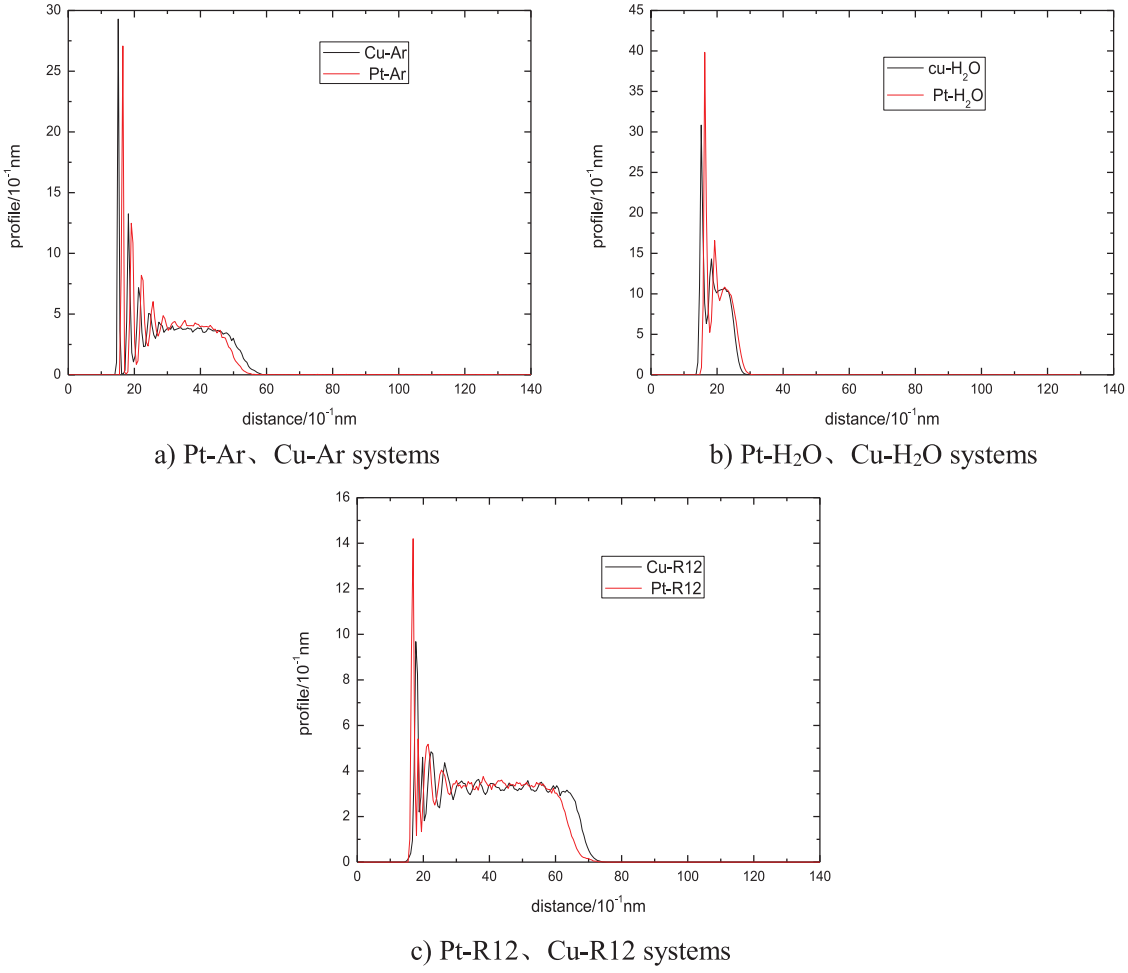

Fig. 11. System density distribution profile along the z direction.

obtained in this paper is slightly higher than the literature values, which may be due to the different statistical methods and details.

3.4. Comparison of interfacial properties

Fig. 10 is the initial structure of Cu-H_2O system obtained by Materials Studio software (MS), and the results of the other systems (Pt-Ar, Pt-H_2O, Pt-R12, Cu-Ar, Cu-R12) are very much the like. There are 500 water molecules. According to the literatures [25–28], density distributions of every system shown in Fig. 11, can be obtained by MS with COMPASS force field [29].

As can be seen from Fig. 11, at the same surface of platinum or copper, the layer number is different for different working fluid. There are 3–4 distinct layers formed near the surface of the metal for the argon flow, and the potential effect of metal wall can be achieved about 1.4 nm far from the wall; for the water and Freon, only 1–2 layers are formed, and potential effect are achieved about 0.6 nm and1.2 nm, respectively.

4. Conclusions

In the paper different water molecule models and solid-liquid potential models are adopted, and a gas-liquid-solid three-phase model is constructed to study the interface characteristics of the water near the wall. By comparative analysis of different models, the following conclusions are obtained.

(1) Density distribution of the water in the near-wall region shows the structure of monomolecular layer at the solid wall; the bubbles near the wall and the droplets in gas phase are observed at higher temperatures.
(2) From the structure of the monomolecular layer on the wall surface, the peak density of monolayer structure of Z-P potential is bigger than that of SH potential; found that the maximum density peak is obtained from the combination: SPC/E and Z-P, and the minimum from the combination: TIP4P and SH;
(3) The predicted fluid density in the gas area is in good agreement with macroscopic value, while in the liquid region it is lower than the macroscopic value, and the deviations increase with increasing temperature; the density values obtained by SPC/E model is closest to refprop; gas-liquid interface width and the condensation coefficient are in accord with the simulation results of the two-phase mode.
(4) At the same surface of platinum or copper, the layer number is different for different working fluid. There are 3–4 distinct layers formed near the surface of the metal for the argon flow, and the potential effect of metal wall can be achieved about 1.4 nm far from the wall; for the water and Freon, only 1–2 layers are formed, and potential effect are achieved about 0.6 nm and1.2 nm, respectively.

Acknowledgement

This work has been supported by the National Natural Science Foundation of China (Grant numbers 51506159).

Referrence

[1] Wang ZJ. Molecular dynamics research and experiment of evaporation and condensation Ph. D. thesis. Beijing: Tsing university; 2002.
[2] Marek R, Straub J. Analysis of the evaporation coefficient and the condensation coefficient of water. Int J Heat Mass Transfer 2001;44:39–53.
[3] Yang TH, Pan C. Molecular dynamics simulation of a thin water layer evaporation and evaporation coefficient. Int J Heat Mass Transfer 2005;48:3516–26.
[4] Yang TH, Pan C, Hsieh HM. Molecular dynamics simulation of interactions between a nano water droplet and an isothermal platinum surface, Nano/Micro engineered and molecular systems, NEMS 2008. In: 3rd IEEE International Conference, Sanya; 2008. p. 1129–33.
[5] Marek R, Straub J. Analysis of the evaporation coefficient and the condensation coefficient of water. Int J Heat Mass Transfer 2001;44:39–53.
[6] Rapaport DC. The art of molecular dynamics simulation. Second ed. Cambridge: Cambridge University Press; 2004.
[7] Xiong JY. Molecular dynamics research on the properties of vapor liquid interface and density maximum of water Master's thesis. Xi'an: Xi'an Jiaotong University; 2006.
[8] Li YS. Molecular dynamics simulation study on flow and heat transfer characteristics in microscale Master's thesis. Xi'an: Xi'an Jiaotong University; 2007.
[9] Torii D, Ohara T. Molecular dynamics study on ultrathin liquid water film sheared between platinum solid walls: liquid structure and energy and momentum transfer. J Chem Phys 2007;126:154706–10.
[10] Kimura T, Maruyama S. Molecular dynamics simulation of water droplet on platinum surface. Nippon Dennetsu Shinpojiumu Koen Ronbunshu 2002;39:393–4.
[11] Spohr E. Computer simulation of the water/platinum interface. J Phys Chem 1989;93:6171–80.
[12] Zhu SB, Philpott MR. Interaction of water with metal surfaces. J Chem Phys 1994;100:6961–8.
[13] Trokhymchuk A, Alejandre J. Computer simulations of liquid/vapor interface in Lennard-Jones fluids: some questions and answers. J Chem Phys 1999;111:8510–23.
[14] Maruyama S, Kimura T, Lu MC. Molecular scale aspects of liquid contact on a solid surface. Thermal Sci Eng 2002;10:23–9.
[15] Kandlikar SG, Steinke ME, Maruyama S, Kimura T. Molecular dynamics simulation and measurement of contact angle of water droplet on a platinum surface. In: Proceedings of IMECEí01:international mechanical engineering congress and exposition; 2001. p. 343–8.
[16] Shi B, Sinha S, Dhir VK. Molecular simulation of the contact angle of water droplet on a platinum surface. In: Proceedings of the 2005 ASME international mechanical engineering congressand exposition, Orlando Florida, USA; 2005.
[17] Zhou WJ, Luan HB, Sun J, He YL, Tao WQ. A Molecular dynamics and lattice boltzmann multiscale simulation for dense fluid flows. Numerical Heat Transf. Part B 2012;61:369–86.
[18] Chen L, Lin H, Tao WQ. Diffusion processes of water and proton in PEM exchange membrane using molecular dynamics simulation. J Eng Thermophys 2010;31:1917–20.
[19] Steinhauser O. Reaction field simulation of wate. Mol Phys 1982;45:335–48.
[20] Chen PF, Chen L, He YL, Tao WQ. A study on the characteristics of liquid interface and condensation process of superheated vapour near a solid wall by molecular dynamics method. Prog Comput Fluid Dyn 2011;11:253–60.
[21] Niu D, Tang G. Static and dynamic behavior of water droplet on solid surfaces with pillar-type nanostructures from molecular dynamics simulation. Int J Heat Mass Transfer 2014;79:647–54.
[22] Liu C, Zhang XM, Tan N, Zeng LD. The thickness and fractional dimension number of the liquid-vapor interface. J Eng Thermophys 2004;25:562–5.
[23] Yang TH, Pan C. Molecular dynamics simulation of a thin water layer evaporation and evaporation coefficient. Int J Heat Mass Transfer 2005;48:3516–26.
[24] Tsuruta T, Tanaka H, Masuoka T. Condensation/evaporation coefficient and velocity distributions at liquid-vapor interface. Int J Heat Mass Transfer 1999;42:4107–16.
[25] Chen L, Lin H, Tao WQ. Molecular dynamics simulation of temperature effect on diffusion process of water and proton in proton exchange membrane. J Xi'an Jiao Tong Univer 2001;45:1–4.
[26] Chen L, Tao WQ. Study on diffusion processes of water and proton in PEM using molecular dynamics simulation. Mater Sci Forum 2012;704-705:1266–72.
[27] Chen L, He YL, Tao WQ. The temperature effect on diffusion processes of water and proton in proton exchange membrane using molecular dynamics simulation. Numer Heat Transfer Part A 2014;65:216–28.
[28] Charati SG, Stern SA. Diffusion of gases in silicone polymers: molecular dynamics simulations. Macromolecules 1998;31:5529–38.
[29] Rigby D, Sun H, Eichinger BE. Computer simulations of poly (ethlene oxides): force field, PVT diagram and cyclization behaviour. Polym Int 1998;44:311–30.